PERFORMANCE IMPROVEMENT OF TAIL ROTORS BY DYNAMICALLY EXTENDABLE CHORD

Haoyun Wan, haoyunwan@nuaa.edu.cn, College of Aerospace Engineering, Nanjing University of Aeronautics and Astronautics, Nanjing 210016, China

Dong Han, donghan@nuaa.edu.cn, College of Aerospace Engineering, Nanjing University of Aeronautics and Astronautics, Nanjing 210016, China

Abstract

In order to study the performance improvement of variable speed tail rotors by dynamically extendable chord, a flight performance model is established, which includes a rotor model, a tail rotor model, a fuselage model, and a propulsive trim method. The flight data of the UH-60A helicopter is utilized to validate this model. The results show that the extendable chord has little effect on the power at hover. At cruise, some extra power is needed. At high speed flight, the power can be reduced significantly. The extendable chord is best placed inboard and close to the blade tip region to efficiently shift the lift and/or the drag inboard. The optimal azimuth angles for the deployment of extendable chord are 40°~50° and 130°~140°. The dynamically extendable chord with non-harmonic motion can obtain more power savings than the other strategies. The extendable chord is suitable for deployment on variable speed tail rotors. When the tail rotor speed is reduced by 20%, the maximum power reduction is 20.3%. The extendable chord increases the maximum thrust, which can compensate for the decrease in the maximum thrust by the reduction of the tail rotor speed.

1. INTRODUCTION

Varying the rotational speed of the main rotor is understood to be an effective means to improve the performance of rotorcraft [1-6]. Changing the engine output shaft speed is one method of changing the main rotor speed, but it will also change the tail rotor speed. The reduction of the tail rotor speed can reduce the tail rotor power in cruise. However, at high speed flight, it can even increase the power required [6]. The tail rotor power required is up to 20% of the main rotor power at the extremes of the flight envelope. The reduction in the tail rotor speed also reduces the maximum thrust of the tail rotor due to the decrease in dynamic pressure, which deteriorates the ability of the tail rotor to balance the main rotor torque and implement the yaw control [7]. It is necessary to compensate for the simultaneous increase in the power and decrease in the maximum thrust.

Rotor blade chord extension can be realized in many ways. One approach is to use a thin extendable trailing-edge plate (TEP), which can be extended through a slit in the blade's trailing edge over a certain spanwise section [8]. Blade chord extension has been extensively explored to improve the helicopter main rotor performance [8-12]. These investigations verified the effectiveness, especially at high gross weight and altitude. Liu et al. studied a static extended trailing edge attached to a NACA0012 airfoil section for achieving lift enhancement with a small drag penalty. It was indicated that the thin extended trailing edge could enhance the lift, whereas the zero-lift drag was not significantly increased [9]. Léon et al. utilized quasi-statically extendable chord sections to expand rotorcraft operating envelope. The results showed that reductions up to 33.4% in the rotor power could be obtained in stall-dominant conditions [10]. Khoshlahjeh and Gandhi explored the benefits of rotor chord extension in stall-dominant conditions. From the simulations in the study, reductions of up to nearly 18% in rotor power requirements were observed with TEP for operation at high gross weight and altitude [8]. Among various blade morphing technologies, the dynamically extendable chord has shown promising in rotor performance improvement for the maximum forward speed and the maximum load capability [11]. Han et al. explored the potential of the static and dynamic extendable chords in reducing the rotor power and improving flight performance. Generally, a lower harmonic extendable chord could save more power than the higher harmonic excitation, and the dynamic chord could reduce the power further than the static [12]. The previous research concentrated on the effect of the extendable chord on the performance of main rotors. However, the potential of the extendable chord in improving the performance of variable speed tail rotors has not yet

been addressed.

The present work provides a comprehensive analysis using a validated helicopter power prediction model to predict performance improvements of variable speed tail rotors with the dynamically extendable chord. The mechanism of the extendable chord enhancing tail rotor performance is explored. The dynamic chord is not limited to 1/rev, and a non-harmonic is also investigated. The benefits of using the extendable chord are explored at reduced tail rotor speed.

2. MODELING METHOD

2.1. Performance prediction method

A helicopter power prediction model is utilized, which includes a main rotor model, a tail rotor model, a fuselage model and a propulsive trim method. The main rotor structural model represents the blades as beams undergoing moderate deflections, and it captures the nonlinear coupling effects between the deformations of advanced helicopter blades. The rigid rotations associated with the blade hinges and the blade rotations about the rotor shaft are introduced as generalized coordinates. Lookup airfoil aerodynamics is utilized. The induced velocity over the rotor disk is predicted by the Pitt-Peters inflow model [13]. Assembling the structural, kinetic, and aerodynamic terms, the equations of motion based on the generalized force formulation can be yielded [14]. The Newmark integration method is utilized to calculate the steady responses in the time domain [15].

The fuselage is treated as a rigid body with aerodynamic forces and moments. Given the initial pitch controls and the rotor shaft attitude angles, the periodic response of the rotor can be obtained for a prescribed forward speed. The hub forces and moments of the main rotor are balanced by the forces and moments acting on the fuselage and tail rotor. These component forces and moments constitute the equilibrium equations of the helicopter, which are solved to update the pitch controls and attitude angles. After iterations of the periodic responses of the rotor, and the solution of the equilibrium equations, the trimmed or converged pitch controls and rotor attitude angles can be obtained. Then, the main rotor power and related information of the helicopter can be derived.

The tail rotor model is based on a rigid beam. The required tail rotor thrust is determined by the main rotor torque divided by the distance from the hub center of the tail rotor to the main rotor shaft. The tail rotor thrust and power are obtained by numerically integrating the blade elements along the blade radius and azimuth with uniform induced velocity [16]. Accounting for the canted angle of tail rotor, the net thrust provided by the tail rotor to counter the main rotor torque can be written as

$$T_{\mathrm{TR}}^{\mathrm{net}} = F_{\mathrm{TR}} T_{\mathrm{TR}} \cos\alpha_{\mathrm{CANT}} \quad (1)$$

where T_{TR} is the tail rotor thrust, α_{CANT} is the canted angle. The tail rotor blockage effects due to the vertical tail are accounted for following the approach of [17-18]. The scaling factor F_{TR} is

$$F_{\mathrm{TR}} = 1 - \frac{3}{4}\frac{S_{\mathrm{FN}}}{S_{\mathrm{TR}}} \quad (2)$$

where S_{FN} is the fin area, S_{TR} is the tail rotor area.

This modeling methodology has been used to analyze the helicopter performance improvement by extendable chord rotors, Gurney flaps, variable speed main rotors and variable speed tail rotors [6, 7, 12].

2.2. Validation

The helicopter model is validated by the flight data of the UH-60A helicopter [19]. The parameters of the main rotor and tail rotor are listed in Table 1 and Table 2 [20-22]. The vertical distance from the mass center of helicopter to the rotor hub is 1.78 m. The fuselage drag force is provided in Ref.19.

The power predictions of the main rotor and tail rotor are compared to the flight test data of the UH-60A at two weight coefficients (C_W = 0.0065, 0.0074) in Fig. 1. The predictions are generally in good agreement with the flight test data, which verifies the application of the present method in analyzing helicopter performance.

Table 1 Parameters of main rotor [20-22].

Parameter	Value
Main rotor radius	8.18 m
Nominal main rotor speed	27.0 rad/s
Blade chord length	0.527 m
Blade twist	Non-linear
Blade Airfoil	SC1095/SC1094R8
Number of blades	4
Flap hinge offset	0.381 m
Blade mass per unit length	13.9 kg/m
Longitudinal shaft tilt	3°

Table 2 Parameters of tail rotor [20-22].

Parameter	Value
Tail rotor radius	1.68 m
Nominal tail rotor speed	124.6 rad/s
Blade chord length	0.25 m
Blade twist	-18°
Blade Airfoil	SC1095
Number of blades	4

Parameter	Value
Tail rotor canted angle	20°
Tail rotor torque arm	9.93 m

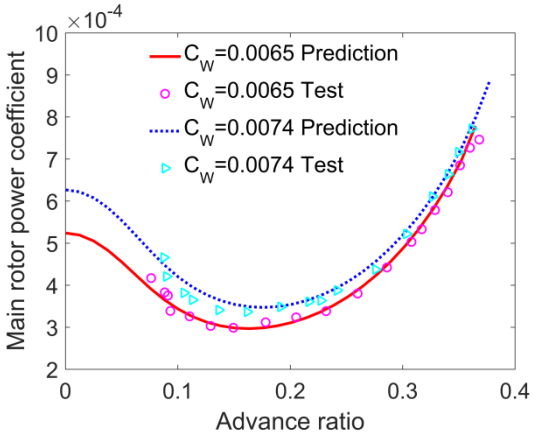

(a) Main rotor power

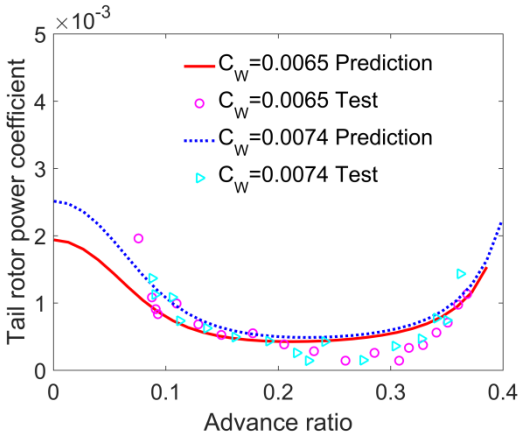

(b) Tail rotor power

Fig. 1 Comparison of the prediction with the flight test data.

2.3. Extendable chord

An extendable chord can change the chord and airfoil camber according to a deployment schedule, as shown in Fig. 2. With a suitable deployment angle (δ = 2° for the SC1094R8 cambered airfoil), the aerodynamic characteristics of the airfoil with a chord extension can remain almost the same [8-12].

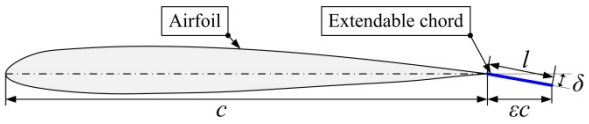

Fig. 2 The configuration of an extendable chord on a cross section.

In this work, we assume that the chord extension does not change the aerodynamic characteristics of the airfoil. The aerodynamics coefficients C_l and C_d with respect to the extendable chord are the same as the baseline coefficients. The aerodynamic coefficients can be nondimensionalized with respect to the baseline blade chord. These coefficients are denoted as $\bar{C}_l$ and $\bar{C}_d$ and are related to those nondimensionalized by the extendable chord as follows:

$$\begin{cases} \bar{C}_l = (1+\varepsilon)C_l \\ \bar{C}_d = (1+\varepsilon)C_d \end{cases} \tag{3}$$

where

$$\varepsilon = l / c \tag{4}$$

where ε represents the chord extension as a percentage of the baseline chord length c. The effect of the chord extension is equivalent to an increase in the aerodynamic coefficients. In fact, the increase in sectional lift comes from an effective chord increase, not a lift coefficient increase.

In the following analyses, the six extendable chords with 10%R (tail rotor radius) as the width (Position 1, 2, 3, 4, 5 and 6) are investigated, as shown in Fig. 3. The start points of the positions are 40%R, 50%R, 60%R, 70%R, 80%R and 90%R.

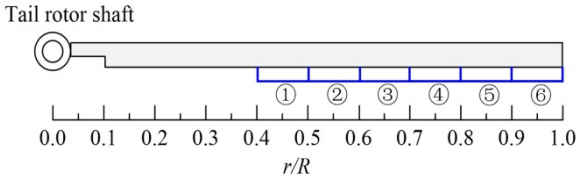

Fig. 3 The configuration of extendable chords in radial direction.

2.4. Power reduction ratio

The power reduction ratio is defined to measure the benefit in tail rotor power saving as

$$\eta = (1 - P / P_b) \times 100\% \tag{5}$$

where P is the tail rotor power to be compared with and P_b is the baseline tail rotor power. The baseline power is defined as the power without any extendable chord. At different rotational speeds, the baseline power varies. In the following analyses, the helicopter baseline flight state is at sea level and a take-off weight of 9474.7 kg (C_W = 0.0074).

3. NOMINAL SPEED TAIL ROTORS

The performance improvements of nominal speed tail rotors with the extendable chord are studied first. The baseline power is defined as the power at 100%Ω (Ω = 124.6 rad/s) without any

extendable chord. The mechanism of the extendable chord improving tail rotor performance is explored.

3.1. Statically extendable chord (SEC)

The extendable chord length is set to be 20% of the blade chord. Fig. 4 explores the effect of the deployment position of the SEC on the tail rotor power reduction. At hover, the extendable chord has little effect on the power reduction. When the extendable chord is placed at position 3, the power reduction is 0.17%. When placed at position 6, it will increase the power instead, and the power increase is 0.06%. At cruise, some extra power is needed for the tail rotor with the SEC. The extendable chord begins to reduce the power when the speed is 205 km/h (position 1). This speed increases as the extendable chord is moved from position 1 to position 6. At high speed flight, the benefit in power saving emerges, and the maximum power reduction is 4.9% at position 4. The power saving at the position 4 is better than at other positions, which indicates that the optimal position for the power reduction is inboard of the blade tip.

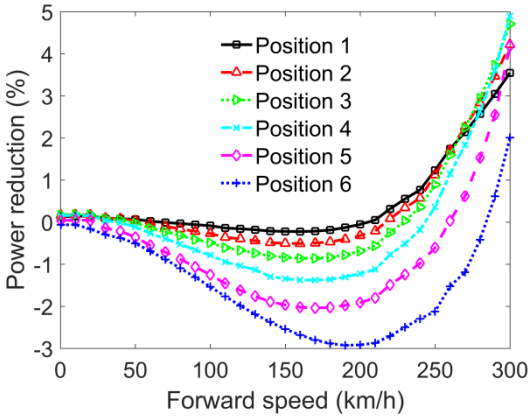

Fig. 4 Power reduction for different position of the SEC.

Fig. 5 shows the distribution of lift and drag of airfoil sections over the tail rotor disk at a speed of 300 km/h. Since tail rotors do not employ cyclic pitch control and cannot achieve the balance of lateral moments, the blades in advancing side generate much more thrust than in retreating side. With the SEC (position 4), lift is generally increased over the annulus from 70% to 80% span (the region where the SEC is present). The SEC also reduces the lift in the outboard regions of the tail rotor disk (outboard of the 70%~80% annulus). The difference in drag over the tail rotor disk between the SEC and the baseline is obvious in advancing side. An increase is generally observed over the annulus from 70% to 80% span. The drag on the outer rim is reduced significantly, which is the primary contributor to the reduction in tail rotor power. The SEC is best placed inboard and close to the blade tip region to efficiently shift the lift and/or the drag inboard.

Fig. 6 shows the distribution of the angle of attack (AoA) over the tail rotor disk with and without the SEC at a speed of 300 km/h. The AoA in advancing side is distinctly larger than that in retreating side. With the SEC (position 4), the AoA generally decreases over the tail rotor disk. The increase in the chord length increases the tail rotor solidity, and more blade area can be used to generate lift. Naturally, it lowers the AoA.

Fig. 7 explores the effect of the azimuth of the extendable chord on the tail rotor power reduction at a speed of 300 km/h. The extendable chord is placed at position 4 with 20% chord extension. The power reduction proportion represents the proportion of the contribution of the local extendable chord (0°~10°, 10°~20°, …, 350°~360°) to the total power reduction per revolution. The tail rotor power reduction with the extendable chord in advancing side is greater than that in retreating side. When the azimuth angles are 40°~50° and 130°~140°, the power reduction can be maximized.

3.2. Dynamically extendable chord (DEC)

For the DEC with 1/rev input, the chord length is prescribed as

$$\varepsilon = A\left[1.0 + \sin(\Omega t + \phi)\right] \tag{6}$$

where, A is the amplitude of input, Ω is the nominal tail rotor speed, and ϕ is the phase of the input.

In the following analysis, the DEC is placed at position 4 with an amplitude of 10%. Fig. 8 presents the effect of the phase of 1/rev input on the tail rotor power and power reduction. At hover and cruise, the change of the power is rather limited. As the forward speed increases, the power reduction can be increased when the phase shifts to a suitable angle. At a speed of 300 km/h, the power reduction can be maximized to be 3.76%, and the corresponding phase is 0°. When the phase is 180°, the power reduction is only 1.30%. The influence of the extendable chord on the power is mainly in advancing side, as shown in Fig. 7. When the phase is 0°, the chord extends out in advancing side, and retracts back in retreating side. It is obvious that the extension of the chord can reduce the AoA over the tail rotor disk and the drag on the outer rim, which leads to the power savings of the tail rotor.

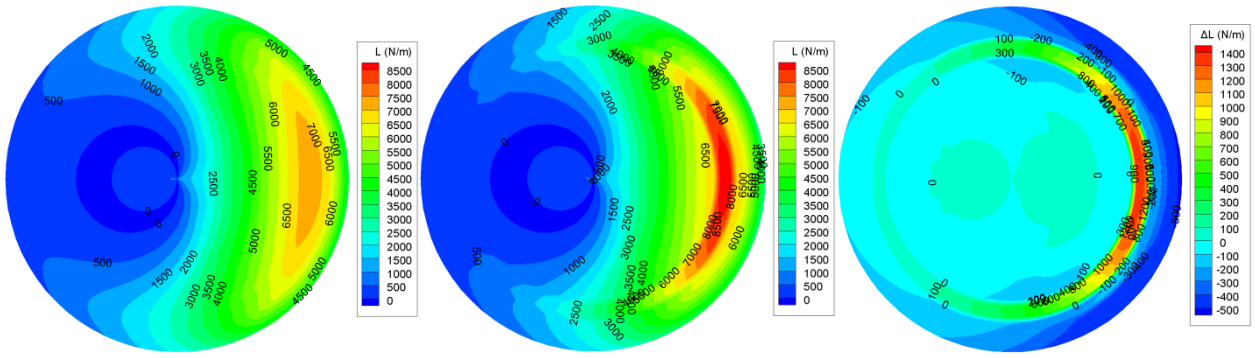

(a) Baseline lift (b) With SEC (c) Lift difference

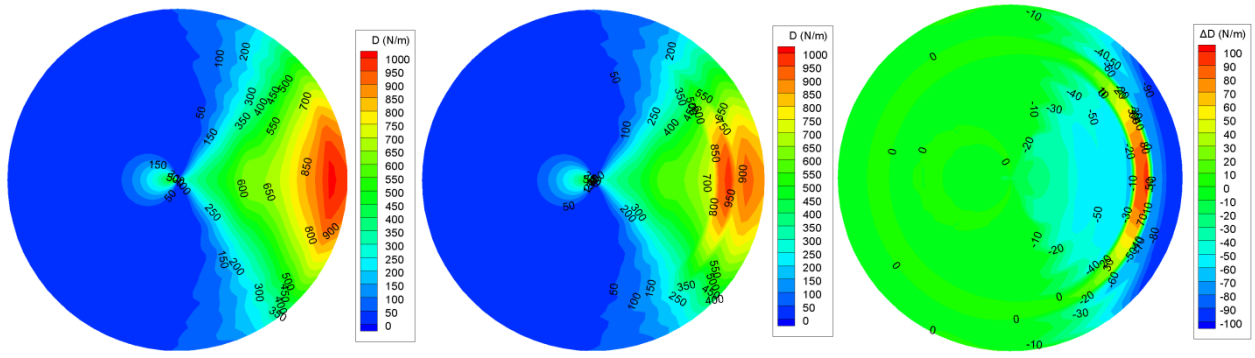

(d) Baseline drag (e) With SEC (f) Drag difference

Fig. 5 Distribution of lift and drag over the tail rotor disk.

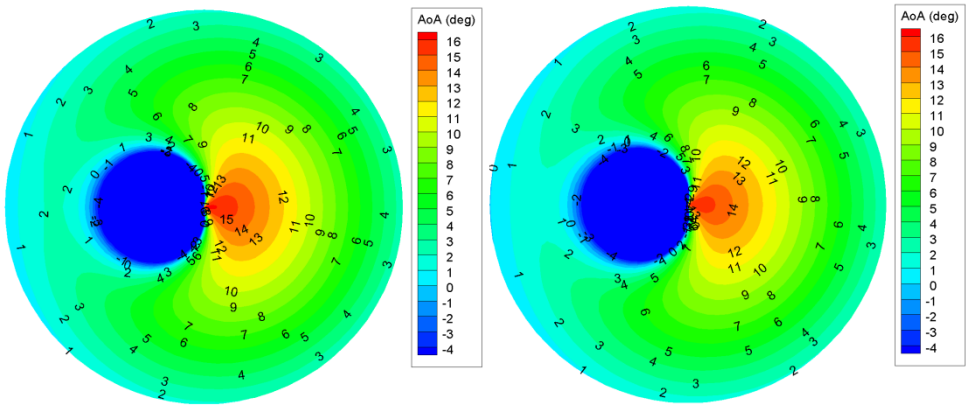

(a) Baseline (b) With SEC

Fig. 6 Distribution of angle of attack over the tail rotor disk.

For the dynamically extendable chord with non-harmonic motion (NDEC), the chord length is prescribed as

$$\varepsilon = \begin{cases} 20\% & (0 \le \psi < 180°) \\ 0 & (180° \le \psi < 360°) \end{cases} \tag{7}$$

where, ψ is the azimuth angle of the tail rotor.

Fig. 9 compares the power reductions for different strategies (SEC, 1/rev DEC, NDEC) of the extendable chord at position 4. For the SEC, the extendable chord length is set to be 10% of the blade chord. For the DEC, the amplitude is 10% and the phase is 0°. At cruise, all three strategies require some extra power (less than 0.68%). At a speed of 300 km/h, the power reductions are 2.55%, 3.76% and 4.20% for the SEC, 1/rev DEC and NDEC, respectively. Under the same conditions, the NDEC can obtain more power savings than the DEC and SEC.

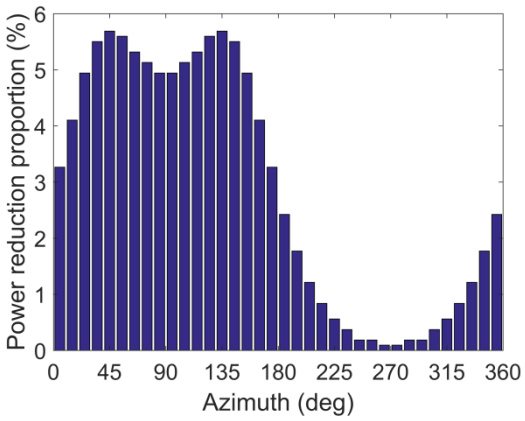

Fig. 7 The proportion of the contribution of the local extendable chord to the total power reduction per revolution.

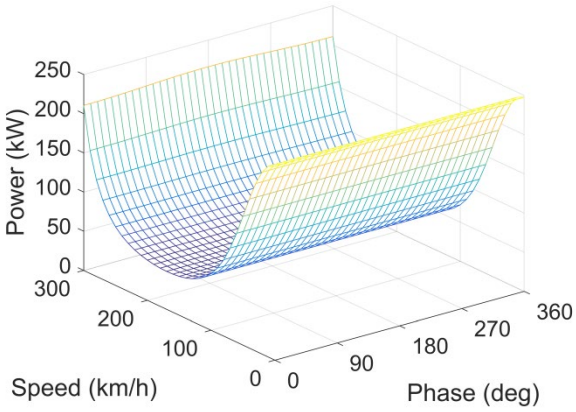

(a) Power

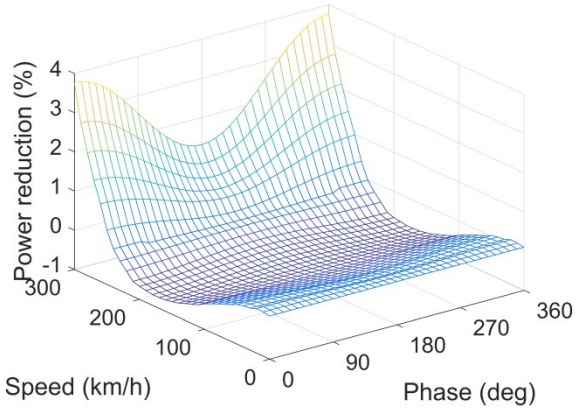

(b) Power reduction

Fig. 8 Power and power reduction for the DEC.

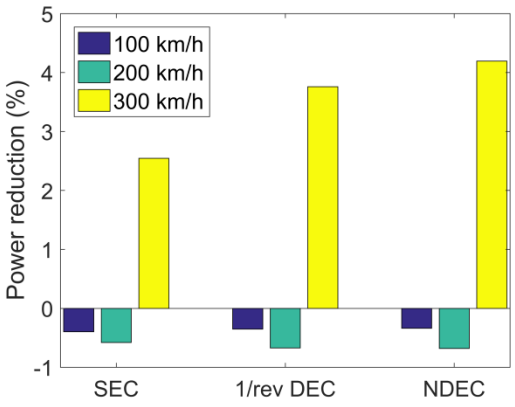

Fig. 9 Power reduction for different strategies of the extendable chord.

4. VARIABLE SPEED TAIL ROTORS

The performance improvements of variable speed tail rotors with the extendable chord are studied. The baseline power is defined as the power at 90%Ω or 80%Ω (Ω = 124.6 rad/s) without any extendable chord. In the following analysis, the benefits of using the NDEC are evaluated at different tail rotor speeds.

Fig. 10 shows the effect of the position of the NDEC on the tail rotor power reduction. It is obvious that the optimal position is the position 5, which is different from that of the NDEC at a rotational speed of 100%Ω (position 4). At high speed flight, the maximum power reductions are 8.45% and 20.3% for the rotational speeds of 90%Ω and 80%Ω, respectively. Compared with the power reduction at 100%Ω, the power reduction at 80%Ω increases significantly. It shows that the extendable chord is suitable for deployment on variable speed tail rotors.

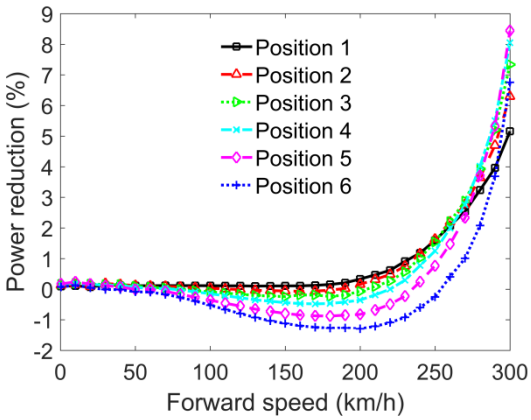

(a) 90%Ω

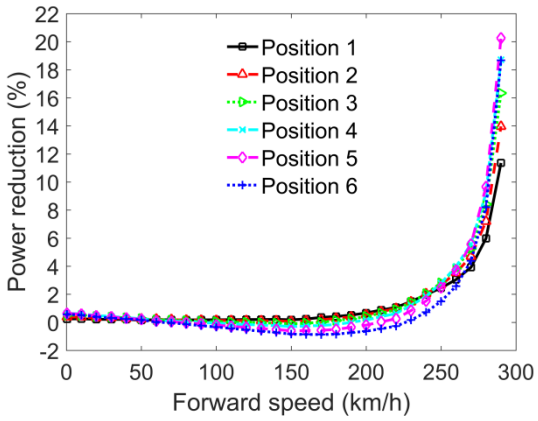

(b) 80%Ω

Fig. 10 Power reduction of variable speed tail rotors for different position of the NDEC.

Fig. 11 shows the thrust required (the solid black line) to balance the main rotor torque, and the maximum thrust for different tail rotor speeds with and without NDEC. The NDEC is placed at position 4. Generally, when the forward flight speed increases, the maximum thrust increases. The reduction in the tail rotor speed causes a reduction in dynamic pressure, which leads to a reduction in the maximum thrust. At a speed of 300 km/h, reducing the speed by 20% almost makes it difficult to implement the yaw control. The extendable chord increases the area of the blades, thereby increasing the maximum thrust, which can compensate for the decrease in the maximum thrust by the reduction of the tail rotor speed.

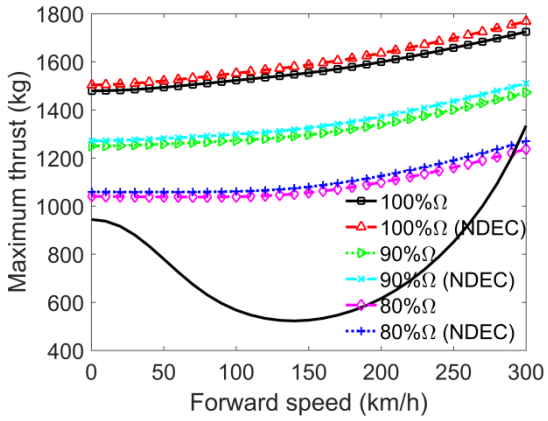

Fig. 11 Maximum thrust of variable speed tail rotors with NDEC.

Fig. 12 shows the distribution of lift, drag and AoA of airfoil sections over the tail rotor disk at different speeds without any extendable chord. At a flight speed of 300 km/h and a rotational speed of 80%Ω, the computation is interrupted due to excessive iterations in tail rotor trim. At reduced tail rotor speed, the most efficient part of the tail rotor blade that generates lift in advancing side moves outboard, and the part with high drag moves inboard. Therefore, the optimal position of the extendable chord moves outboard. Since the drag and AoA increase significantly with the reduction in tail rotor speed, the extendable chord appears to be effective in reducing the power of reduced speed tail rotors.

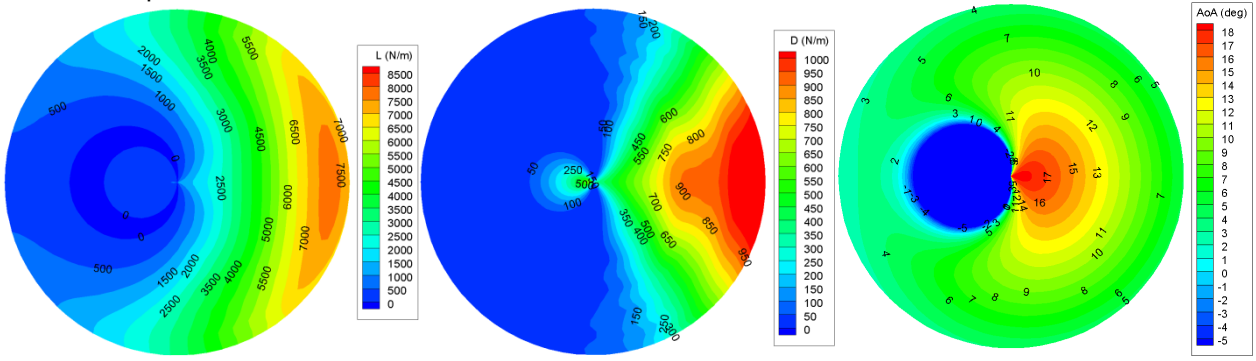

(a) Lift (90%Ω, 300 km/h) (b) Drag (90%Ω, 300 km/h) (c) AoA (90%Ω, 300 km/h)

Presented at 47th European Rotorcraft Forum, United Kingdom, 7-9th September, 2021

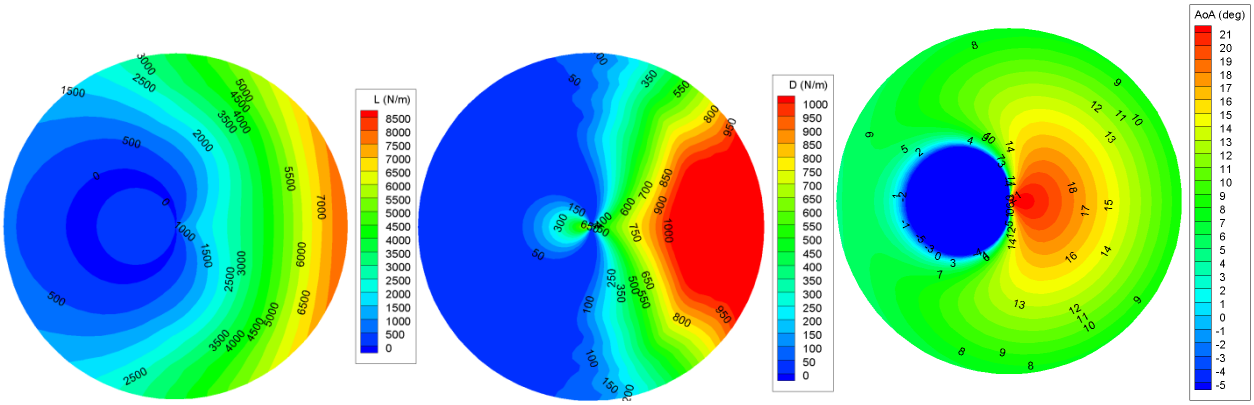

(d) Lift (80%Ω, 290 km/h) (e) Drag (80%Ω, 290 km/h) (f) AoA (80%Ω, 290 km/h)

Fig. 12 Distribution of lift, drag and AoA over the tail rotor disk at different speeds.

5. CONCLUSIONS

This work used a validated helicopter power prediction model to predict performance improvements of variable speed tail rotors with the dynamically extendable chord. The performance analyses yielded the following conclusions:

1) At hover, the statically extendable chord (SEC) has little effect on the power reduction. At cruise, some extra power is needed for the tail rotor with the SEC. At high speed flight, the benefit in power saving emerges, and the maximum power reduction is 4.9% at 70%~80% annulus.

2) The lift is generally increased in the area where the SEC is present and reduced in the outboard regions. The drag is also generally increased in the same area. The drag on the outer rim is reduced significantly, which is the primary contributor to the reduction in tail rotor power. The SEC is best placed inboard and close to the blade tip region to efficiently shift the lift and/or the drag inboard.

3) With the SEC, the angle of attack generally decreases over the tail rotor disk. The increase in the chord length increases the tail rotor solidity, and more blade area can be used to generate lift. Naturally, it lowers the angle of attack and delays stall.

4) The tail rotor power reduction with the extendable chord in advancing side is greater than that in retreating side. When the azimuth angles for the deployment of extendable chord are 40°~50° and 130°~140°, the power reduction can be maximized.

5) With the dynamically extendable chord (DEC), the maximum power reduction is 3.76%, and the corresponding phase is 0°. The dynamically extendable chord with non-harmonic motion (NDEC) can obtain more power savings than the other strategies. Under the same conditions (300 km/h, 70%~80% annulus, 10% chord length) the power reductions are 2.55%, 3.76% and 4.20% for the SEC, 1/rev DEC and NDEC, respectively.

6) The extendable chord is suitable for deployment on variable speed tail rotors. At high speed flight, the maximum power reductions are 8.45% and 20.3% for the rotational speeds of 90%Ω and 80%Ω, respectively.

7) The reduction in the tail rotor speed causes a reduction in dynamic pressure, which leads to a reduction in the maximum thrust. The extendable chord increases the area of the blades, which can increase the maximum thrust.

8) At reduced tail rotor speed, the most efficient part of the tail rotor blade that generates lift in advancing side moves outboard, and the part with high drag moves inboard. Therefore, the optimal position of the extendable chord moves outboard. Since the drag and angle of attack increase significantly as the tail rotor speed decreases, the extendable chord can effectively reduce the power.

ACKNOWLEDGMENTS

This work is supported from the National Natural Science Foundation of China (11972181), the Open Research Foundation of the Key Rotor Aerodynamics Laboratory (2005RAL20200104) and the Six Talent Peaks Project in Jiangsu Province (GDZB-013).

REFERENCES

[1] Prouty, R. W., “Should we consider variable rotor speeds?,” Vertiflite, Vol. 50, No. 4, 2004, pp. 24-27.

[2] Steiner, J., Gandhi F., Yoshizaki Y., “An investigation of variable rotor RPM on performance and trim,” Proceedings of the American Helicopter Society 64th Annual Forum, American Helicopter Soc. International,

Alexandria, VA, April 29–May 1, 2008, pp. 697-705.
[3] DiOttavio, J., Friedmann, D., “Operational benefit of an optimal, widely variable speed rotor,” Proceedings of the American Helicopter Society 66th Annual Forum, American Helicopter Soc. International, Alexandria, VA, May 11-13, 2010, pp. 1865-1871.
[4] Mistry, M., Gandhi, F., “Helicopter performance improvement with variable rotor radius and RPM,” Journal of the American Helicopter Society, Vol. 59, No. 4, 2014, pp. 17–35.
[5] Bowen-Davies, G. M., Chopra, I., “Aeromechanics of a Slowed Rotor,” Journal of the American Helicopter Society, Vol. 60, No.3, 2015 , pp. 1-13.
[6] Han, D., Barakos. G. N., “Variable-speed tail rotors for helicopters with variable-speed main rotors,” The Aeronautical Journal, Vol.121, No. 1238, 2017, pp. 433-448.
[7] Dong, C., Han, D., Yu, L., “Performance analysis of variable speed tail rotors with Gurney flaps,” Chinese Journal of Aeronautics, Vol. 31, No. 11, 2018, pp. 2104-2110.
[8] Khoshlahjeh, M., Gandhi, F., “Extendable chord rotors for helicopter envelope expansion and performance improvement,” Journal of the American Helicopter Society, Vol. 59, No. 1, 2014, pp. 1-10.
[9] Liu, T., Montefort, J., Liou, W., et al, “Lift enhancement by static extended trailing edge,” Journal of Aircraft, Vol. 44, No. 6, 2007, pp. 1939-1947.
[10] Léon, O., Hayden, E., Gandhi, F., “Rotorcraft operating envelope expansion using extendable chord sections,” Proceedings of the American Helicopter Society 65th Annual Forum, American Helicopter Soc. International, Alexandria, VA, May 27-29, 2009, pp. 1940-1953.
[11] Kang, H., Saberi, H., Gandhi, F., “Dynamic blade shape for improved helicopter rotor performance,” Journal of the American Helicopter Society, Vol. 55, No. 3, 2010, pp. 1-11.
[12] Han, D., Yang, K., Barakos, G. N., “Extendable chord for improved helicopter rotor performance,” Aerospace Science and Technology, Vol. 80, 2018, pp. 445-451.
[13] Peters, D. A., Haquang, N., “Technical Note: Dynamic inflow for practical applications”, Journal of the American Helicopter Society, Vol. 33, No. 4, 1988, pp. 64-68.
[14] Han, D., Smith, E. C., “Lagwise loads analysis of a rotor blade with an embedded chordwise absorber,” Journal of Aircraft, Vol. 46, No. 4, 2012, pp. 1280-1290.
[15] Owen D. R. J., Hinton E., Finite elements in plasticity: theory and practice, Pineridge Press, Swansea, 1980, pp. 431-436.
[16] Leishman, J. G., Principles of Helicopter Aerodynamics, 2nd ed., Cambridge Univ. Press, Cambridge, New York, USA, 2006.
[17] Padfield, G. D., Helicopter flight dynamics: the theory and application of flying qualities and simulation modeling, 2nd, Blackwell Publishing Ltd, Oxford, 2007, pp. 142-146.
[18] Lynn, R. R., Robinson, F. D., Batra, N. N., et al, “Tail rotor design part I: Aerodynamics”, Journal of the American Helicopter Society, Vol. 15, No. 4, 1970, pp. 2-15.
[19] Yeo, H., Bousman, W. G., Johnson, W., “Performance analysis of a utility helicopter with standard and advanced rotors,” Journal of the American Helicopter Society, Vol. 49, No. 3, 2004, pp. 250-270.
[20] Hilbert, K. B., “A mathematical model of the UH-60 helicopter,” Technical Report NASA-TM-85890, 1984.
[21] Buckanin, R. M., Herbst, M. K., Lockwood, R. A., et al, “Airworthiness and flight characteristics test of a sixth year production UH-60A,” USAAEFA Project No. 83-24, California: United States Army Aviation Engineering Flight Activity, Edwards Air Force Base, 1985.
[22] Nagata, J. I., Piotrowski, J. L., Young, C. J., et al, “Baseline performance verification of the 12th year production UH-60A black hawk helicopter,” USAAEFA Project No. 87-32, California: United States Army Aviation Engineering Flight Activity, Edwards Air Force Base, 1989.